Transmit Beamforming Design for Noncoherent Distributed Integrated Sensing and Communication Systems

Kawon Han
University College London
London, United Kingdom
kawon.han@ucl.ac.uk

Kaitao Meng
University College London
London, United Kingdom
kaitao.meng@ucl.ac.uk

Christos Masouros
University College London
London, United Kingdom
c.masouros@ucl.ac.uk

***Abstract*—This paper presents a transmit beamforming design for distributed integrated sensing and communication (D-ISAC) systems. The proposed noncoherent D-ISAC system consists of multiple ISAC nodes that collaborate to perform both sensing and communication tasks without requiring phase-level synchronization. It utilizes coordinated multi-point (CoMP) transmission to enable the communication task. For sensing, the system takes advantage of both collocated and distributed multi-input multi-output (MIMO) radars to localize targets by estimating the angle-of-arrival (AOA) and time-of-flight (TOF). To design the transmit beamforming for the D-ISAC system, we adopt the Cramer-Rao bound (CRB) as the sensing performance metric for target localization, while using the signal-to-interference-plus-noise ratio (SINR) as the metric for communication performance. We then formulate a D-ISAC beamforming design problem that minimizes the localization CRB while ensuring a minimum SINR level for each communication user. Numerical simulations demonstrate the performance gains of the proposed noncoherent D-ISAC system, highlighting improved CRB-SINR trade-offs compared to conventional single-node ISAC systems.**

***Index Terms*—Coordinated multipoint (CoMP), Cramér-Rao bound (CRB), distributed integrated sensing and communication (D-ISAC), multi-input multi-output (MIMO) radar, transmit beamforming.**

I. Introduction

With the growing demand for wireless resources, integrated sensing and communication (ISAC) technologies have attracted significant attention in both academic and industrial sectors [1]. ISAC systems offer considerable benefits over the separate deployment of communication and radar systems by utilizing unified hardware and shared resources, enabling dual radar-communication functionality. This integrated approach leads to improved efficiency in spectral usage, reduced hardware costs, and lower energy consumption.

Recent advancements in ISAC have largely focused on signal design [1], [2] and resource allocation [3], [4] within single-node systems, which typically employ monostatic sensing links and single-station communication services. However, fewer studies have explored distributed ISAC (D-ISAC) systems, which involve cooperation between multiple ISAC nodes or base stations (BSs). In general, the distributed systems can leverage multiple communication and sensing links while mitigating inter-node interference, presenting new opportunities for enhancing ISAC performance. By utilizing the distributed nature of multiple ISAC nodes, D-ISAC systems can expand communication coverage and provide more accurate target parameter estimation. Recent research has examined the performance of network-level cooperative ISAC, addressing aspects such as spatial resource allocation [5], cooperative cluster sizes [6], and antenna-to-BS allocation [7]. These studies have demonstrated the performance gains achievable through cooperation among multiple ISAC nodes, underscoring the potential of networked ISAC systems.

Despite the promising potential of D-ISAC systems, few studies have delved into signal design and related signal processing techniques for D-ISAC systems. Consequently, the performance gains from the cooperation remain underutilized. For instance, recent work on single-node transmit beamforming has explored multi-static sensing using distributed sensing receivers, though it did not consider distributed transmission [8]. In [9], transmit beamforming in distributed cloud radio access networks (C-RAN) integrated with rate-splitting multiple access was proposed, leveraging only angle-of-arrival (AOA) information for target localization. Similarly, in [10], a coordinated transmit beamforming design was introduced to address distributed sensing and multi-user communication, with inter-cell interference taken into account. However, this work did not explore the potential sensing gains achievable through signal-level fusion in distributed multi-input multi-output (MIMO) radar systems. Thus, the systematic properties newly introduced in D-ISAC systems have to be considered to design the transmit signal, which have not been explored yet.

From a practical system perspective, this work investigates a noncoherent D-ISAC system without phase-level synchronization, where all ISAC nodes are connected to a central processing unit (CPU). The system employs coordinated multi-point (CoMP) transmission for communication and leverages both collocated and distributed MIMO radars for sensing, using angle-of-arrival (AOA) and time-of-flight (TOF) estimation to localize targets. Based on this setup, we propose a transmit beamforming design framework that addresses the trade-offs between sensing and communication (S&C) performance in

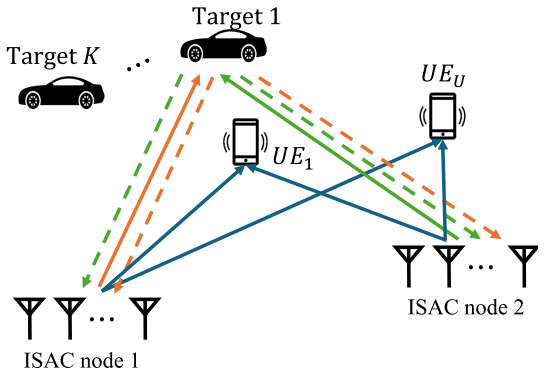

(a)

Fig. 1: System setup illustration for D-ISAC, showcasing CoMP transmission for downlink communication and target localization using distributed MIMO radar.

noncoherent D-ISAC systems. The main contributions of this work are summarized as follows:

- We propose a noncoherent D-ISAC system that operates without phase-level synchronization, using both TOF and AOA information to localize targets, while employing CoMP transmission for serving communication users.
- We formulate the transmit beamforming design problem for D-ISAC, minimizing the Cramer-Rao bound (CRB) for target localization in noncoherent distributed MIMO radar systems, while maintaining a minimum signal-to-interference-plus-noise ratio (SINR) for communication users.
- We analyze the trade-offs between sensing and communication performance in the proposed noncoherent D-ISAC system, demonstrating the effects of system parameters and localization methods, as well as comparisons with single-node ISAC systems.

II. System Model

A. Distributed ISAC System

In a distributed ISAC system including N ISAC nodes, each ISAC node consists of M_t transmit antennas and M_r receive antennas. The n^{th} node is located at the position of $\mathbf{p}_n = [x_n, y_n]^T$ in two-dimensional Cartesian coordination with respect to the reference origin. All networked ISAC nodes cooperatively cover U communication users using CoMP transmission, as shown in Fig. 1. Assuming that all ISAC nodes employ orthogonal frequency-division multiplexing (OFDM) with L subcarriers and share transmitted signals with each other, they are all in active mode and are time-frequency synchronized without phase-level synchronization. Consequently, they function as a distributed MIMO radar system, jointly detecting and estimating K targets. The received signals from all ISAC nodes are transmitted to a central processing unit (CPU) to fuse the sensing information for target localization.

To ensure sufficient degree-of-freedoms (DOFs) in the sensing waveform for multiple targets, we introduce a weighted summation of multi-user communication and MIMO radar signals as the ISAC transmit signal [11]. Using the frequency-domain representation of OFDM signals, the transmitted signal of the single OFDM symbol can be expressed as

$$\mathbf{X}_n = \mathbf{W}_{c,n}\mathbf{S}_c + \mathbf{W}_{r,n}\mathbf{S}_{r,n}, \tag{1}$$

where $\mathbf{W}_{c,n} \in \mathrm{C}^{M_t \times U}$ and $\mathbf{S}_c \in \mathrm{C}^{U \times L}$ represent a precoding matrix and desired data symbol for multi-user communication, respectively. $\mathbf{W}_{r,n} \in \mathrm{C}^{M_t \times M_t}$ and $\mathbf{S}_{r,n} \in \mathrm{C}^{M_t \times L}$ represent a MIMO radar beamforming matrix and a radar signal respectively at the node n for multi-target sensing. Here, we assume the uncorrelated conditions for communication and radar signals satisfying $\mathrm{E}[\mathbf{S}_c\mathbf{S}_c^H] = \mathbf{I}_U$, $\mathrm{E}[\mathbf{S}_{r,n}\mathbf{S}_{r,n}^H] = \mathbf{I}_{M_t}$, and $\mathrm{E}[\mathbf{S}_c\mathbf{S}_{r,n}^H] = \mathbf{0}_{U \times M_t}$.

B. Communication Signal Model

According to the system description, each ISAC node transmits a dual-functional signal for both radar sensing and downlink communication. We assume that N distributed ISAC nodes serve U users, each equipped with a single antenna. Let $\mathbf{y}_{c,u}$ denote the received signal at user u, which is expressed as

$$\begin{aligned}\mathbf{y}_{c,u} &= \sum_{n=1}^{N} \mathbf{h}_{n,u}^H \mathbf{X}_n + \mathbf{z}_{c,u}, \\ &= \sum_{n=1}^{N} \left(\mathbf{h}_{n,u}^H \mathbf{w}_{c,n,u}\mathbf{s}_{c,u} + \sum_{i=1, i\neq u}^{U} \mathbf{h}_{n,u}^H \mathbf{w}_{c,n,i}\mathbf{s}_{c,i} \right) \\ &\qquad + \sum_{n=1}^{N} \mathbf{h}_{n,u}^H \mathbf{W}_{r,n}\mathbf{S}_{r,n} + \mathbf{z}_{c,u}\end{aligned} \tag{2}$$

where $\mathbf{h}_{n,u}^H$ represents the channel vector between user u and the n^{th} ISAC node and $\mathbf{z}_{c,u}$ represents a circularly symmetric complex Gaussian noise following $\mathcal{CN}(0, \sigma_c^2)$. Additionally, $\mathbf{w}_{c,n,u}$ and $\mathbf{s}_{c,u}$ expresses a precoding vector and transmit data symbol for the user u. In (2), the second and third terms are regarded as the integrated multi-user and radar interference from all ISAC nodes.

C. Sensing Signal Model

For cooperative sensing, the received signal at N nodes includes both mono-static and bi-static scatterings from K targets. Given that M_r receiving antennas are arranged in a uniform linear array with half-wavelength spacing, the received sensing signal at the n^{th} ISAC node, transmitted from the m^{th} node, is expressed as

$$\mathbf{Y}_{s,n,m} = \sum_{k=1}^{K} b_{n,m}^k \mathbf{a}_r(\theta_n^k) \left(\mathbf{a}_t^T(\theta_m^k)\mathbf{X}_m \odot \mathbf{d}^T(\tau_{n,m}^k) \right), \tag{3}$$

where $\odot$ represents the hadamard product. Also, $\mathbf{a}_r(\theta) = \left[1, e^{j\frac{2\pi}{\lambda}d_0 \sin\theta}, \ldots, e^{j\frac{2\pi}{\lambda}(M_r-1)d_0 \sin\theta}\right]^T$ and $\mathbf{a}_t(\theta) = \left[1, e^{j\frac{2\pi}{\lambda}d_0 \sin\theta}, \ldots, e^{j\frac{2\pi}{\lambda}(M_t-1)d_0 \sin\theta}\right]^T$ are the receive and transmit steering vectors, and $\mathbf{d}(\tau) = \left[1, e^{-j2\pi\frac{B}{L}\tau}, e^{-j2\pi\frac{B}{L}2\tau}, \ldots, e^{-j2\pi\frac{B}{L}(L-1)\tau}\right]^T$

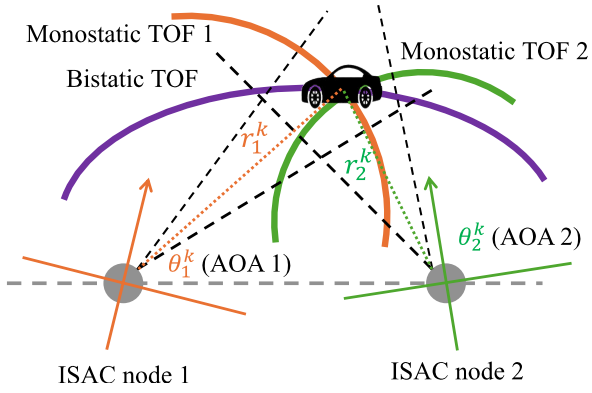

(a)

Fig. 2: Target localization in D-ISAC using joint TOF and AOA parameters.

represents the delay steering vector, where λ is the wavelength of the operating frequency and B is the signal bandwidth. Furthermore, $b_{n,i}^k$ and $\tau_{n,i}^k = \tau_n^k + \tau_i^k$ represent a complex amplitude and a time-of-flight (TOF) from the i^{th} node, to the k^{th} target to the n^{th} node, respectively. θ_n^k denotes an angle of the target seen from the n^{th} node. Additionally, let $\mathbf{q}_k = [x_k, y_k]^T$ denote the position of target k. Then, both TOF and angle of the target are a function of the target location as follows:

$$\tau_n^k = \frac{\sqrt{(x_k - x_n)^2 + (y_k - y_n)^2}}{c}, \tag{4a}$$

$$\theta_n^k = \arctan 2(y_k - y_n, x_k - x_n), \tag{4b}$$

where c is the speed of light.

From (3), the received signal at the node n is rewritten as

$$\mathbf{Y}_{s,n} = \mathbf{A}_{r,n} \sum_{m=1}^{N} \left(\mathbf{B}_{n,m} \mathbf{V}_{n,m}^T\right) + \mathbf{Z}_{s,n} \tag{5}$$

where $\mathbf{V}_{n,m} = \mathbf{X}_m^T \mathbf{A}_{t,m} \odot \mathbf{D}_{n,m}$. The remaining matrices are expressed as $\mathbf{A}_{r,n} = \left[\mathbf{a}_r(\theta_n^1), \mathbf{a}_r(\theta_n^2), \ldots, \mathbf{a}_r(\theta_n^K)\right]$, $\mathbf{A}_{t,n} = \left[\mathbf{a}_t(\theta_n^1), \mathbf{a}_t(\theta_n^2), \ldots, \mathbf{a}_t(\theta_n^K)\right]$, $\mathbf{B}_{n,m} = \text{diag}(b_{n,m}^1, b_{n,m}^2, \ldots, b_{n,m}^K)$, and $\mathbf{D}_{n,m} = \left[\mathbf{d}(\tau_{n,m}^1), \mathbf{d}(\tau_{n,m}^2), \ldots, \mathbf{d}(\tau_{n,m}^K)\right]$. Also, $\mathbf{Z}_{s,n}$ represents a circularly symmetric complex Gaussian noise with each entry following $\mathcal{CN}(0, \sigma_n^2)$. Here, we assume that all nodes have the same noise variance $\sigma_n^2 = \sigma^2$. Accordingly, the sensing task in the distributed ISAC system is to estimate target locations $\mathbf{q}_k$ using the collected signals from all nodes $\mathbf{Y}_s = [\mathbf{Y}_{s,1}^T, \mathbf{Y}_{s,2}^T, ..., \mathbf{Y}_{s,N}^T]^T$.

III. Performance Metric for Distributed ISAC

A. Communication Performance Metric

As a communication performance metric for transmit beamforming design, we utilize the signal-to-interference-plus-noise ratio (SINR). From (2), we derive the SINR for a typical user u in the case of noncoherent cooperation in the distributed ISAC system. In noncoherent CoMP transmission, the distributed ISAC nodes are not phase-synchronized. As a result, the received signal at the typical communication user is a noncoherently combined signal from the jointly transmitted communication signals. Based on this assumption and the received signal model (2), the SINR for the u^{th} communication user in noncoherent CoMP can be expressed as [12]

$$\gamma_{c,u}^{\text{nc}} = \frac{\sum_{n=1}^{N} |\mathbf{h}_{n,u}^H \mathbf{w}_{c,n,u}|^2}{\sum_{n=1}^{N} \left[\sum_{i \neq u}^{U} |\mathbf{h}_{n,u}^H \mathbf{w}_{c,n,i}|^2 + \|\mathbf{h}_{n,u}^H \mathbf{W}_{r,n}\|_F^2\right] + \sigma_c^2}. \tag{6}$$

The denominator addresses the multi-user and radar signal interference from all ISAC nodes.

B. Sensing Performance Metric

For a sensing performance metric, we exploit CRB of target localization in the distributed ISAC nodes. The target parameters and localization method are illustrated in Fig. 2, which leverages both TOF and AOA information by fully exploiting the characteristics of distributed and collocated MIMO radar systems. Let $\mathbf{\Psi}$ denote the collection of all the real-valued unknown parameters given as

$$\mathbf{\Psi} = [\boldsymbol{\theta}^T, \boldsymbol{\tau}^T, \mathbf{b}_{\text{R}}^T, \mathbf{b}_{\text{I}}^T]^T \in \mathbb{R}^{(2KN + 2KN^2) \times 1}, \tag{7}$$

where $\boldsymbol{\theta} = [\theta_1^1, \theta_1^2, \ldots, \theta_n^k, \ldots, \theta_N^K]^T \in \mathbb{R}^{KN \times 1}$, $\boldsymbol{\tau} = [\tau_1^1, \tau_1^2, \ldots, \tau_n^k, \ldots, \tau_N^K]^T \in \mathbb{R}^{KN \times 1}$, and $\mathbf{b} = [b_{1,1}^1, b_{1,1}^2, \ldots, b_{n,i}^k, \ldots, b_{N,N}^K]^T \in \mathbb{C}^{KN^2 \times 1}$ with $\mathbf{b}_{\text{R}} = \text{Re}(\mathbf{b}), \mathbf{b}_{\text{I}} = \text{Im}(\mathbf{b})$. Since both $\boldsymbol{\theta}$ and $\boldsymbol{\tau}$ contribute to localize targets in Cartesian coordination as (4a) and (4b), we can alternatively define the vector of unknown parameter as

$$\mathbf{\Theta} = [\mathbf{x}^T, \mathbf{y}^T, \mathbf{b}_{\text{R}}^T, \mathbf{b}_{\text{I}}^T]^T \in \mathbb{R}^{(2KN^2 + 2K) \times 1}, \tag{8}$$

where $\mathbf{x} = [x_1, x_2, \ldots, x_K]^T \in \mathbb{R}^{K \times 1}$ and $\mathbf{y} = [y_1, y_2, \ldots, y_K]^T \in \mathbb{R}^{K \times 1}$.

The joint log-likelihood function of the observation $\mathbf{Y}_s$ conditioned on $\mathbf{\Psi}$ is given by [13]

$$\mathcal{L}(\mathbf{Y}_s | \mathbf{\Psi}) = -\sum_{n=1}^{N} \left\| \mathbf{Y}_{s,n} - \mathbf{A}_{r,n} \sum_{m=1}^{N} \left(\mathbf{B}_{n,m} \mathbf{V}_{n,m}^T\right) \right\|_F^2 + c_0, \tag{9}$$

where c_0 is some constant. Then, the Fisher Information matrix (FIM) with respect to $\mathbf{\Psi}$ is expressed as

$$\mathbf{F}(\mathbf{\Psi}) = \mathbb{E}\left[\left(\frac{\partial}{\partial \mathbf{\Psi}} \mathcal{L}(\mathbf{Y}_s | \mathbf{\Psi})\right)\left(\frac{\partial}{\partial \mathbf{\Psi}} \mathcal{L}(\mathbf{Y}_s | \mathbf{\Psi})\right)^T\right]. \tag{10}$$

To obtain the FIM with respect to target localization parameters $\mathbf{\Theta}$, we adopt the chain rule as follows:

$$\mathbf{F}(\mathbf{\Theta}) = \mathbf{J} \mathbf{F}(\mathbf{\Psi}) \mathbf{J}^T, \tag{11}$$

where $\mathbf{J} = \frac{\partial \mathbf{\Psi}}{\partial \mathbf{\Theta}}$ and $\mathbf{J}$ is the Jacobian matrix, which represents the partial derivatives of $\mathbf{\Psi}$ with respect to $\mathbf{\Theta}$. Finally, we get the sensing metric related to the target localization CRB, which is expressed as

$$\text{CRB} = \text{tr}\left([\mathbf{F}(\mathbf{\Theta})]^{-1}\right). \tag{12}$$

The Jacobian matrix for the noncoherent combination is derived as

$$\mathbf{J}_{\text{nc}} = \begin{bmatrix} \frac{\partial \boldsymbol{\theta}}{\partial \mathbf{x}} & \frac{\partial \boldsymbol{\tau}}{\partial \mathbf{x}} & \mathbf{0} & \mathbf{0} \\ \frac{\partial \boldsymbol{\theta}}{\partial \mathbf{y}} & \frac{\partial \boldsymbol{\tau}}{\partial \mathbf{y}} & \mathbf{0} & \mathbf{0} \\ \mathbf{0} & \mathbf{0} & \mathbf{I}_{KN^2} & \mathbf{0} \\ \mathbf{0} & \mathbf{0} & \mathbf{0} & \mathbf{I}_{KN^2} \end{bmatrix}. \tag{13}$$

Although the detailed derivation of the FIM $\mathbf{F}(\boldsymbol{\Psi})$ is omitted here for brevity, the readers can refer to [13], [14] for further details.

IV. D-ISAC Transmit Beamforming Design

A. Problem Formulation

We propose a transmit beamforming design framework for noncoherent D-ISAC system. Compared to the transmit beamforming design for the monostatic ISAC system [15], the target localization performance depends on both TOF and AOA of targets in the D-ISAC system. Based on communication and sensing performance metrics discussed in section III-A and section III-B, the goal of the transmit beamforming design for noncoherent D-ISAC is to minimize the localization CRB under the communication SINR constraint for each downlink user. Accordingly, we develop the following optimization problem under the per-antenna power constraint.

$$\underset{\mathbf{W}_{c,n},\mathbf{W}_{r,n}}{\text{minimize}} \quad \text{tr}\left([\mathbf{F}(\boldsymbol{\Theta})]^{-1}\right) \tag{14a}$$

$$\text{subject to} \quad \gamma_{c,u}^{\text{nc}} \geq \Gamma_c, \ \forall u, \tag{14b}$$

$$[\mathbf{R}_{nn}]_{m,m} \leq P_T, \ \forall n, m, \tag{14c}$$

where $\mathbf{R}_{nn} = \mathbf{X}_n \mathbf{X}_n^H$. The objective function (14a) addresses the target localization performance. Also, (14b) describes the minimum communication SINR of each user, which determines the trade-off between communication and sensing performances. (14c) is the per-antenna power constraint in all ISAC nodes.

B. D-ISAC Transmit Beamforming Design Using SDR

We can simply rewrite problem (14) using the Schur complement as

$$\underset{\mathbf{W}_{c,n},\mathbf{W}_{r,n},t_i}{\text{minimize}} \quad \sum_{i=1}^{2K+2KN^2} t_i \tag{15a}$$

$$\text{subject to} \quad \begin{bmatrix} \mathbf{F} & \mathbf{e}_i \\ \mathbf{e}_i^T & t_i \end{bmatrix} \succeq 0, \ \forall i \in \{1, 2, \cdots, 2K + 2KN^2\}, \tag{15b}$$

$$\gamma_{c,u}^{\text{nc}} \geq \Gamma_c, \ \forall u, \tag{15c}$$

$$[\mathbf{R}_{nn}]_{m,m} \leq P_T, \ \forall n, m, \tag{15d}$$

where $\mathbf{e}_i$ represents the i^{th} column of the identity matrix $\mathbf{I}_{(2K+2KN^2)}$. We express the FIM matrix as $\mathbf{F}$ to simplify the notation. Since the problem (15) is non-convex, it can be relaxed to a convex problem using semi-definite relaxation (SDR).

Firstly, dropping out the range steering vector and referring to [15], it can be readily observed that each block matrix of the FIM matrix is a linear function of $\tilde{\mathbf{R}} = \tilde{\mathbf{X}}\tilde{\mathbf{X}}^H$, where $\tilde{\mathbf{X}} = \left[\mathbf{X}_1^T, \mathbf{X}_2^T, ..., \mathbf{X}_N^T\right]^T$. This is represented as

$$\tilde{\mathbf{R}} = \begin{bmatrix} \mathbf{R}_{11} & \mathbf{R}_{12} & \cdots & \mathbf{R}_{1N} \\ \mathbf{R}_{21} & \mathbf{R}_{22} & \cdots & \mathbf{R}_{2N} \\ \vdots & \vdots & \ddots & \vdots \\ \mathbf{R}_{N1} & \mathbf{R}_{N2} & \cdots & \mathbf{R}_{NN} \end{bmatrix}, \tag{16}$$

where $\mathbf{R}_{ij} = \mathbf{X}_i \mathbf{X}_j^H$. Then, we further simplify the beamforming design by applying the orthogonal condition to the radar signal $\mathbf{S}_{r,1}, \mathbf{S}_{r,2}, \ldots, \mathbf{S}_{r,N}$ such that $\text{E}[\mathbf{S}_{r,i}\mathbf{S}_{r,j}^H] = \mathbf{0}_{M_t \times M_t}, \forall i \neq j$. Also, using the uncorrelated property of communication and radar signals, the communication SINR constraint in (6) can be rewritten as

$$\gamma_{c,u}^{\text{nc}} = \frac{\sum_{n=1}^{N} \mathbf{h}_{n,u}^H \mathbf{R}_{c,n,u} \mathbf{h}_{n,u}}{\sum_{n=1}^{N} \mathbf{h}_{n,u}^H \mathbf{R}_{nn} \mathbf{h}_{n,u} - \sum_{n=1}^{N} \mathbf{h}_{n,u}^H \mathbf{R}_{c,n,u} \mathbf{h}_{n,u} + \sigma_c^2} \tag{17}$$

where $\mathbf{R}_{c,n,u} = \mathbf{w}_{c,n,u}\mathbf{w}_{c,n,u}^H$ is the rank-1 matrix. Since off-diagonal block matrices in (16) does not affect the communication SINR constraint and the radar signals at different nodes are orthogonal each other, the variables are reduced to only the block diagonal matrix of (16) consisting of $\mathbf{R}_{nn}, n = 1, 2, ..., N$.

Substituting (17) into (15c) and dropping the rank-1 constraint out, the problem (15) can be recast as

$$\underset{\mathbf{R}_{c,n,u},\mathbf{R}_{r,n},t_i}{\text{minimize}} \quad \sum_{i=1}^{2K+2KN^2} t_i \tag{18a}$$

$$\text{s.t.} \quad \begin{bmatrix} \mathbf{F} & \mathbf{e}_i \\ \mathbf{e}_i^T & t_i \end{bmatrix} \succeq 0, \ \forall i \in \{1, 2, \cdots, 2K + 2KN^2\}, \tag{18b}$$

$$\mathbf{R}_{nn} = \mathbf{R}_{r,n} + \sum_{u=1}^{U} \mathbf{R}_{c,n,u}, \tag{18c}$$

$$[\mathbf{R}_{nn}]_{m,m} \leq P_T, \ \forall n, m, \tag{18d}$$

$$\mathbf{R}_{c,n,u} \succeq 0, \ \forall u, \ \mathbf{R}_{nn} - \sum_{u=1}^{U} \mathbf{R}_{c,n,u} \succeq 0, \tag{18e}$$

$$\sum_{n=1}^{N} \left[\left(1 + \frac{1}{\Gamma_c}\right) \mathbf{h}_{n,u}^H \mathbf{R}_{c,n,u} \mathbf{h}_{n,u} - \mathbf{h}_{n,u}^H \mathbf{R}_{nn} \mathbf{h}_{n,u} \right] \geq \sigma_c^2, \ \forall u. \tag{18f}$$

The relaxed problem is now convex, which can be solved by MATLAB's CVX solver. In (18), the number of variables to be designed is $(U+1)M_t^2 N$ in total.

After obtaining the optimal solution of the relaxed problem, we retrieve the suboptimal solution for beamforming matrices $\mathbf{W}_{c,n}$ and $\mathbf{W}_{r,n}$. Similar to [11], the obtained solution of (18) can be exploited to compute the rank-1 solutions and its corresponding beamforming vectors as follows:

$$\hat{\mathbf{w}}_{c,n,u} = \left(\mathbf{h}_{n,u}^H \mathbf{R}_{c,n,u} \mathbf{h}_{n,u}\right)^{-1/2} \mathbf{R}_{c,n,u} \mathbf{h}_{n,u} \tag{19}$$

Also, the radar beamforming matrix $\hat{\mathbf{W}}_{r,n}$ is obtained via Cholesky decomposition of $\mathbf{R}_{r,n}$.

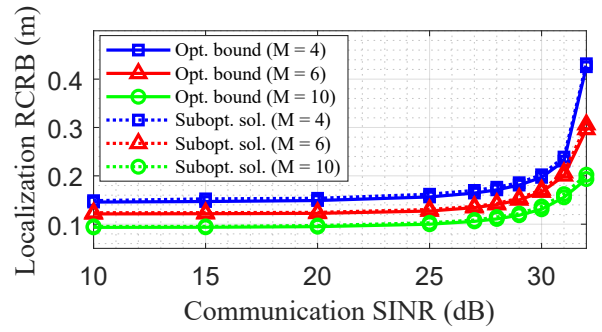

(a)

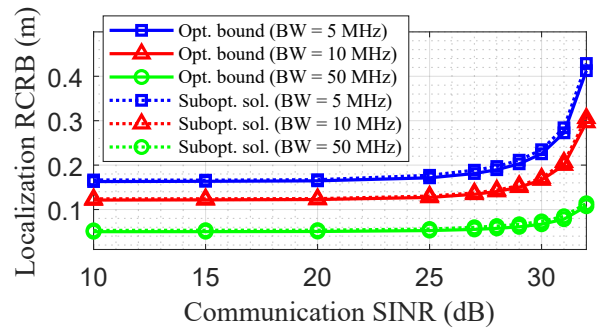

(b)

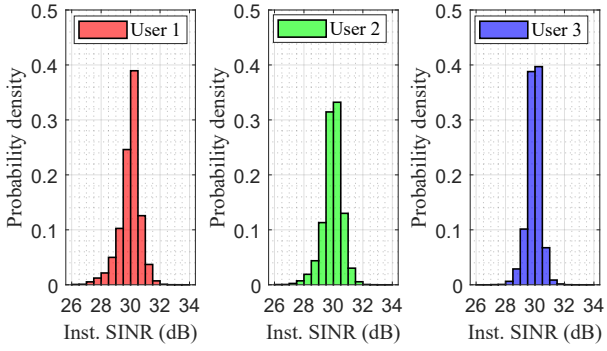

(c)

Fig. 3: Performance of the noncoherent D-ISAC system with the proposed transmit beamforming: (a) CRB-SINR trade-offs for different numbers of transmit antennas, (b) CRB-SINR trade-offs for varying signal bandwidths, and (c) instantaneous SINR distribution at a 30 dB SINR threshold.

V. Simulation Results

In this section, we present simulation results that demonstrate the performance of the proposed transmit beamforming design in the D-ISAC system. The results focus on the trade-off between sensing and communication performance, specifically the CRB-SINR trade-off. First, we validate the performance of the noncoherent D-ISAC system based on the proposed beamforming design in scenarios involving multiple targets and users. For the simulations, two ISAC nodes ($N = 2$) are positioned at $\mathbf{p}_1 = [-141.4\ m, 141.4\ m]^T$ and $\mathbf{p}_2 = [-141.4\ m, -141.4\ m]^T$, each equipped with a 16-element receive array ($M_r = 16$). The default number of transmit antennas is $M_t = M = 6$, and the default bandwidth is 10 MHz. The two ISAC nodes collaboratively estimate the positions of two targets ($K = 2$), located at $[-65\ m, 25\ m]^T$ and $[50\ m, 5\ m]^T$, while serving three communication users ($U = 3$) positioned at $[-160\ m, -40\ m]^T$, $[150\ m, -25\ m]^T$, and $[0\ m, -150\ m]^T$. For the system setup, the number of OFDM subcarriers is 16 with QPSK modulation, target SNR $P_T \sum_{k=1}^{2} \sum_{n=1}^{2} \sum_{m=1}^{2} |\beta_{n,m}^k|^2/\sigma^2$ is set to 0 dB, and $P_T/\sigma_c^2 = 20$ dB.

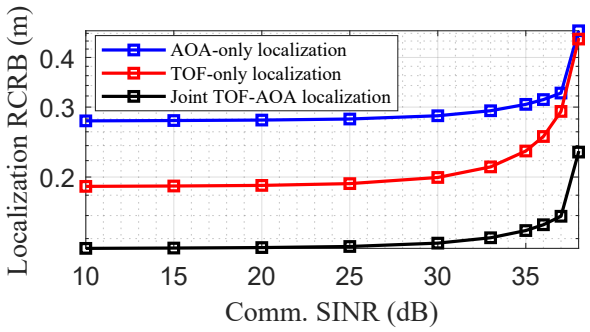

(a)

Fig. 4: Comparisons of CRB-SINR trade-offs for AOA-only, TOF-only, and joint TOF-AOA localization methods.

Fig. 3 shows the performance trade-offs between communication SINR and localization CRB under various system parameters. Both the optimal bound obtained by (18) and the suboptimal solutions from (19) are plotted for comparison. To examine the effect of the number of transmit antennas, we scale the per-antenna power constraint P_T relative to the case of $M = 6$, ensuring that total power remains constant. As expected, the CRB-SINR bound improves as the number of antennas increases, allowing the system to achieve better localization and communication performance through the beamforming gain, as shown in Fig. 3(a). Additionally, increasing the bandwidth results in improved localization performance, as illustrated in Fig. 3(b). This is because larger bandwidth enhances the accuracy of TOF estimation, which is utilized for target localization in distributed MIMO radar systems [13]. Furthermore, the results indicate that the suboptimal solution closely follows the optimal bound, validating the tightness of the SDR-based beamforming design. Fig. 3(c) shows the probability density of instantaneous SINR for three different users obtained from 1000 Monte Carlo simulations, with the SINR threshold set to 30 dB. The results show that all users experience similar SINR distributions, with slight variations. This implies that the instantaneous SINR may vary due to the block-level precoding with an average SINR constraint, which could be further enhanced by using symbol-level precoding as in [16].

In Fig. 4, we compare localization performance when using only AOA, only TOF, and the joint use of both AOA and TOF information. For this simulation, a single user and a single target are positioned at $[-50\ m, 0\ m]^T$ and $[50\ m, 0\ m]^T$, respectively. As expected, joint TOF-AOA localization outper-

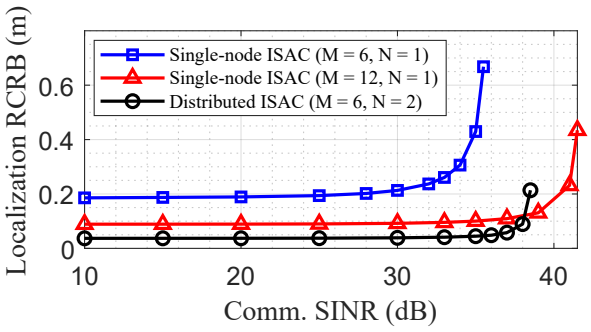

(a)

Fig. 5: Comparison of CRB-SINR trade-offs between single-node ISAC systems ($M = 6, N = 1$ and $M = 12, N = 1$) and the D-ISAC system ($M = 6, N = 2$).

forms both AOA-only and TOF-only localization approaches across the range of communication SINR values. The joint approach maximizes the resources of the D-ISAC, utilizing all monostatic and bistatic TOF observations in distributed MIMO radar and angle estimations from each node in the collocated MIMO radar. This underscores that D-ISAC systems introduce new systematic properties that should be considered in designing the transmit signal. Note that the performance illustrated in Fig. 4 may vary based on signal bandwidth and the number of antennas.

Fig. 5 illustrates the localization CRB-SINR trade-offs for both single-node and D-ISAC systems. Two configurations are shown for single-node ISAC ($M = 6, N = 1$ and $M = 12, N = 1$), along with a distributed ISAC system with $M = 6$ antennas and $N = 2$ nodes. The D-ISAC system outperforms both single-node setups, particularly compared to the single-node ISAC with $M = 12$. This result highlights the advantages of deploying distributed ISAC nodes in terms of improved sensing performance due to spatial diversity and additional bistatic links. However, the communication SINR performance is lower in the noncoherent D-ISAC setup than in the single-node ISAC with the same total number of antennas, as the single-node ISAC system provides a coherent gain equivalent to $M = 12$.

The simulation results confirm that the proposed noncoherent D-ISAC system with SDR-based beamforming design significantly enhances both sensing and communication performance. Increasing the number of antennas, bandwidth, and leveraging joint TOF-AOA information improves the target localization accuracy. Additionally, the distributed nature of the ISAC nodes provides performance gains over conventional single-node ISAC systems.

VI. Conclusion

In this paper, we proposed a transmit beamforming design framework for D-ISAC systems, allowing multiple ISAC nodes to collaboratively perform communication and sensing tasks without phase-level synchronization. The formulated problem balances the trade-off between sensing and communication performance, using the target localization CRB, based on both TOF and AOA parameters, as the sensing metric, and SINR for communication. Numerical simulations demonstrate that the proposed noncoherent D-ISAC framework leveraging joint TOF-AOA information significantly extends the sensing-communication trade-offs compared to conventional single-node ISAC systems. Future work includes exploring coherent D-ISAC systems with phase-level synchronization and analyzing the effects of synchronization on overall system performance.

References

[1] F. Liu, Y. Cui, C. Masouros, J. Xu, T. X. Han, Y. C. Eldar, and S. Buzzi, "Integrated sensing and communications: Toward dual-functional wireless networks for 6G and beyond," *IEEE Journal on Selected Areas in Communications*, vol. 40, no. 6, pp. 1728–1767, 2022.

[2] F. Liu, L. Zhou, C. Masouros, A. Li, W. Luo, and A. Petropulu, "Toward dual-functional radar-communication systems: Optimal waveform design," *IEEE Transactions on Signal Processing*, vol. 66, no. 16, pp. 4264–4279, 2018.

[3] I. Valiulahi, C. Masouros, and A. Salem, "Net-zero energy dual-functional radar-communication systems," *IEEE Transactions on Green Communications and Networking*, vol. 7, no. 1, pp. 356–369, 2023.

[4] F. Dong, F. Liu, Y. Cui, W. Wang, K. Han, and Z. Wang, "Sensing as a service in 6G perceptive networks: A unified framework for ISAC resource allocation," *IEEE Transactions on Wireless Communications*, vol. 22, no. 5, pp. 3522–3536, 2022.

[5] K. Meng, C. Masouros, A. P. Petropulu, and L. Hanzo, "Cooperative ISAC Networks: Opportunities and Challenges," *IEEE Wireless Communications*, pp. 1–8, 2024.

[6] K. Meng, C. Masouros, G. Chen, and F. Liu, "Network-Level Integrated Sensing and Communication: Interference Management and BS Coordination Using Stochastic Geometry," *IEEE Transactions on Wireless Communications*, pp. 1–1, 2024.

[7] K. Meng, K. Han, C. Masouros, and L. Hanzo, "Network-level ISAC: Performance Analysis and Optimal Antenna-to-BS Allocation," *arXiv preprint arXiv:2410.06365*, 2024.

[8] X. Lou, W. Xia, S. Jin, and H. Zhu, "Beamforming Optimization in Distributed ISAC System with Integrated Active and Passive Sensing," *IEEE Transactions on Communications*, 2024.

[9] P. Gao, L. Lian, and J. Yu, "Cooperative ISAC with direct localization and rate-splitting multiple access communication: A pareto optimization framework," *IEEE Journal on Selected Areas in Communications*, vol. 41, no. 5, pp. 1496–1515, 2023.

[10] X. Yang, Z. Wei, J. Xu, Y. Fang, H. Wu, and Z. Feng, "Coordinated Transmit Beamforming for Networked ISAC with Imperfect CSI and Time Synchronization," *IEEE Transactions on Wireless Communications*, 2024.

[11] X. Liu, T. Huang, N. Shlezinger, Y. Liu, J. Zhou, and Y. C. Eldar, "Joint transmit beamforming for multiuser MIMO communications and MIMO radar," *IEEE Transactions on Signal Processing*, vol. 68, pp. 3929–3944, 2020.

[12] R. Tanbourgi, S. Singh, J. G. Andrews, and F. K. Jondral, "A tractable model for noncoherent joint-transmission base station cooperation," *IEEE Transactions on Wireless Communications*, vol. 13, no. 9, pp. 4959–4973, 2014.

[13] H. Godrich, A. M. Haimovich, and R. S. Blum, "Target localization accuracy gain in MIMO radar-based systems," *IEEE Transactions on Information Theory*, vol. 56, no. 6, pp. 2783–2803, 2010.

[14] J. Li, L. Xu, P. Stoica, K. W. Forsythe, and D. W. Bliss, "Range compression and waveform optimization for MIMO radar: A Cramér–Rao bound based study," *IEEE Transactions on Signal Processing*, vol. 56, no. 1, pp. 218–232, 2007.

[15] F. Liu, Y.-F. Liu, A. Li, C. Masouros, and Y. C. Eldar, "Cramér-Rao bound optimization for joint radar-communication beamforming," *IEEE Transactions on Signal Processing*, vol. 70, pp. 240–253, 2021.

[16] N. Babu, C. Masouros, C. B. Papadias, and Y. C. Eldar, "Precoding for multi-cell ISAC: from coordinated beamforming to coordinated multipoint and bi-static sensing," *arXiv preprint arXiv:2402.18387*, 2024.